

## Differential elastic electron scattering cross sections for ethane in the energy range from 2 to 100 eV

H Tanaka<sup>†</sup>, L Boesten<sup>‡</sup>, D Matsunaga<sup>‡||</sup> and T Kudo<sup>§</sup>

<sup>†</sup> Department of General Sciences, Sophia University, Chiyoda-ku, Tokyo 102, Japan

<sup>‡</sup> Department of Physics, Sophia University, Chiyoda-ku, Tokyo 102, Japan

<sup>§</sup> Department of Electrical Engineering, Sophia University, Chiyoda-ku, Tokyo 102, Japan

Received 1 December 1987

**Abstract.** Cross sections for vibrationally elastic scattering of the system e-C<sub>2</sub>H<sub>6</sub> have been measured with a newly constructed apparatus of the crossed-beam type using the relative flow technique. Absolute elastic differential cross sections for C<sub>2</sub>H<sub>6</sub> were obtained by measuring the ratios to the cross section for He at impact energies of 2, 3, 4, 5, 6, 7.5, 8.5, 10, 15, 20, 40 and 100 eV and angles from 15° to 130°. Integral and momentum transfer cross sections were calculated from the DCS and are compared with other measurements. A short description of the apparatus is given.

### 1. Introduction

A broad maximum centred around 7.5 eV in the total cross sections is a common feature of scattering by the electron-saturated hydrocarbon molecules CH<sub>4</sub>, C<sub>2</sub>H<sub>6</sub> and C<sub>3</sub>H<sub>8</sub>, and their cross sections increase with increasing molecular size.

Within the framework of a systematic determination of the absolute differential cross sections (DCS) for the vibrationally elastic and inelastic scattering of electrons from CH<sub>4</sub> (Tanaka *et al* 1982, 1983) and C<sub>2</sub>H<sub>6</sub> (Matsunaga *et al* 1981), we have previously published a broad range of quantitative DCS for the e-CH<sub>4</sub> system over the angular range from 30° to 140° for 3 to 20 eV. There, it was confirmed that below 7.5 eV, the angular distribution is characteristic of the d wave of a weak <sup>2</sup>T<sub>2</sub> resonance. In a preliminary investigation of the e-C<sub>2</sub>H<sub>6</sub> system the angular dependence of the DCS near 7.5 eV (Matsunaga *et al* 1981) appeared to be that of a short-lived shape resonance with a dominant f-wave behaviour.

This was confirmed by Curry *et al* (1985) who reported vibrationally elastic and inelastic scattering DCS for CH<sub>4</sub> and C<sub>2</sub>H<sub>6</sub> in the energy range from 7.5 to 20 eV at scattering angles from 30° to 140°. For the normalisation of their cross sections they referred to our unpublished data (Matsunaga *et al* 1981) and concluded that the appearance of a short-lived shape resonance (d wave for CH<sub>4</sub> and f wave for C<sub>2</sub>H<sub>6</sub>) is consistent with our measurement as well as with other previous measurements (Rohr 1980). A few theoretical papers on CH<sub>4</sub> have appeared (Gianturco and Thompson 1976, 1980, Abusalbi *et al* 1983), however, up to the present no theoretical calculations for C<sub>2</sub>H<sub>6</sub> are available.

<sup>||</sup> Now at: Fujitsu Corporation, 1015 Kami-Odanaka, Nakahara-ku, Kawasaki-shi, Japan.

In the meantime, we have re-measured the DCS of  $C_2H_6$  with a new improved vacuum system and a spectrometer which was carefully fine-tuned to reduce various systematic errors. On the theoretical side, Kimura *et al* (1987) have begun tests on the continuum multiple-scattering method to calculate the total and differential cross sections for  $e-C_2H_6$ .

In this paper, we report the absolute DCS of  $C_2H_6$  at electron impact energies from 2 to 100 eV for the angular range from  $15-20^\circ$  to  $130^\circ$ . We describe the new apparatus and experimental method in some detail in § 2 and present the results in § 3.

## 2. Experimental

### 2.1. Apparatus

The apparatus is similar to that used by Trajmar *et al* at JPL with crossed electron and molecular beams. Energy discrimination is performed by single hemispherical electrostatic dispersion elements of mean radius  $r_0 = (49.5 + 34.5)/2$  mm for both the monochromator and analyser. The latter can be rotated around the scattering centre from  $-10^\circ$  to  $+135^\circ$ . The electron energy and the shape of the incident electron beam as well as the electron-optical properties of the analyser system are determined by a series of tube lenses following Chutjian's design (1979). The driving voltages of these lens systems were calculated with a matrix transfer program using the  $\{a\}$  parameters of DiChio and Natali (1974). However, because of poor performance of the instrument, all voltages were re-evaluated with the help of a newly written ray-tracing program following the proposals of Kisker (1983) and Kisker *et al* (1982), and have led to a considerably improved resolution and constancy of the transmission function. The programs are described elsewhere (Boesten 1988). Rational function fits to the sweeping voltages are used to set up a look-up table of stepping voltages in the memory of a personal computer controlling the lens voltages (at present an NEC 8001). The incident electron energy, the scattered electron energy (i.e. energy loss) and two focusing voltages of the zoom lens preceding the analyser are swept during the measurements in increments corresponding to the 10–20 meV steps in the impact energy.

Molecular or atomic beams are produced either from tube nozzles (0.3–0.6 mm inner diameter), capillary arrays, or high-temperature crucibles. The height of the nozzle can be adjusted from outside the vacuum chamber for optimum intersection of electron beam, molecular beam, and view cone of the analyser (about 2.5 mm above the nozzle).

Pulses from the channeltron multiplier are amplified, shaped and amplitude limited by a single-channel analyser, accumulated in a Canberra 8100 multichannel analyser (MCA), and transmitted to an up-counting digital display and a rate meter for initial gun and lens adjustments. The MCA connects to an NEC 9800 personal computer for read-out, display and data storage. This allows an almost instantaneous and enlarged inspection of the shape of the elastic peak for fine tuning of the instrument.

All electron lens elements, beam defining apertures and nozzles are made of molybdenum, the various elements being insulated by sapphire balls and here and there by machinable ceramic. The vacuum chamber consists of non-magnetic stainless steel and is evacuated by a 6 in oil diffusion pump with a liquid nitrogen trap. The monochromator and analyser (both within boxes) are differentially pumped by a turbomolecular pump to reduce the deleterious effects of corrosive gases and instabilities in the gun due to changes in the space charge distribution. The ultimate

vacuum is in the high  $10^{-8}$  Torr range with the gas beam off, and  $5\text{--}10 \times 10^{-6}$  Torr with the gas beam on, while the pressure in the housing of the monochromator remains below  $2 \times 10^{-6}$  Torr (estimated). Magnetic fields in the region of the spectrometer are reduced to less than 5 mG by a permalloy shield (2 mm) enclosed in the vacuum chamber.

The overall instrumental resolution is typically 30–40 meV for an incident electron beam intensity of  $2\text{--}20 \times 10^{-9}$  A and impact energies from 2 to 100 eV and is fairly constant (e.g. 3–4 days: 31 meV at 100 eV, disilane). The impact energy scale was calibrated against the 19.37 eV resonance of He. This translates into an effective contact potential of +0.33 eV arising between the molybdenum parts and the stainless steel surrounding the collision region. Ray-tracing calculations have shown that the electron beam is about 1.5–2.5 mm wide depending on the impact energy. With an estimated gas beam diameter of 1.5 mm and the aperture-defined view cone of the analyser entrance ( $\pm 3^\circ$ ), the angular resolution is estimated as about  $\pm 1.5^\circ$ . As long as the molecular beam remains within the view cone of the analyser, the detection probability for scattered electrons should be uniform.

The spectrometer contains two features not used in the present experiment, i.e. provision for a double hemispherical analyser and a third differential pump with a cold finger to absorb the molecular beam.

## 2.2. Cross section calibration

The relative flow method has been described in detail by Srivastava *et al* (1975) and Trajmar and Register (1985) and will be discussed only briefly. It relies on the measurement of the ratio of elastically scattered intensities ( $I_x$ ) of  $C_2H_6$  to that of He ( $I_h$ ). 'Providing the measurement is performed under identical experimental conditions for both gases, and the flow in the nozzle is collisionless', the ratio of the two cross sections  $\sigma_x$  and  $\sigma_h$  can be determined from the following simple equation

$$\frac{\sigma_x}{\sigma_h} = \frac{I_x P_h}{I_h P_x} \quad (1)$$

where  $P_x$  and  $P_h$  are the corresponding back pressures (measured with a Baratron capacitance manometer). The absolute value of the cross sections of  $C_2H_6$  is then obtained by multiplication by the well established and readily available absolute cross sections of He.

Special care was taken to avoid systematic errors.

(i) The axes of electron source and analyser were aligned with the help of a laser beam. The beam can be passed through a small hole in the sphere of the monochromator and the collimating apertures in the exit lens and forms a spot of about 0.4 mm diameter at the scattering region. A small drill is inserted into the nozzle and the monochromator box is aligned until the projection of the beam onto a far away screen shows a symmetric pattern of interference produced from both sides of the drill. Then the analyser box is adjusted so that the light reflected from the drill shows a uniform intensity at all angles when viewed through the apertures and sphere (hole) of the analyser input. A poor alignment of the axes can also be recognised in a known DCS by a 'rotation' of the shape, i.e. by an increase of about 10% in the low-angle regions and a similar drop at high angles for a particular example.

(ii) Initially, a capillary array was used because of its superior collimation properties (cf Brinkmann and Trajmar 1981). However, in spite of a very careful demagnetisation *in loco*, it was found that the stainless steel tubes retain some residual magnetism

which is strong enough to deflect a low-energy electron beam ( $<10$  eV). This was observed as variations in the current of a Faraday cup when the nozzle was raised or lowered. The phenomenon disappears when the capillary array is replaced. Thus, in the final measurements, a molybdenum nozzle with an aspect ratio of 0.04 (diameter/length) was used.

(iii) The back pressures, e.g. 7.5 Torr for He and 1.3 Torr for  $C_2H_6$ , were adjusted so as to obtain nearly identical Knudsen numbers for both gases. Only then can one assume an approximately similar intensity distribution in the gas beam (cf Olander and Kruger 1970). Failure to observe the correct Knudsen number results in systematic intensity errors of the measured DCS since equation (1) becomes invalid.

To assess the above effects as well as the effect of the newly calculated lens- and gun-driving voltages more clearly, extensive measurements of the DCS of Ar (Tanaka and Boesten 1988) were performed and compared with published values. A further check of the alignment during measurements consists in drawing a normalised graph of the measured He cross sections and comparing this with the shape of the 'Brinkmann curves' (figure 4 of Brinkmann and Trajmar 1981). In our experience, distortions in this graph are a sure indicator of misalignment in the beams.

### 3. Results and discussion

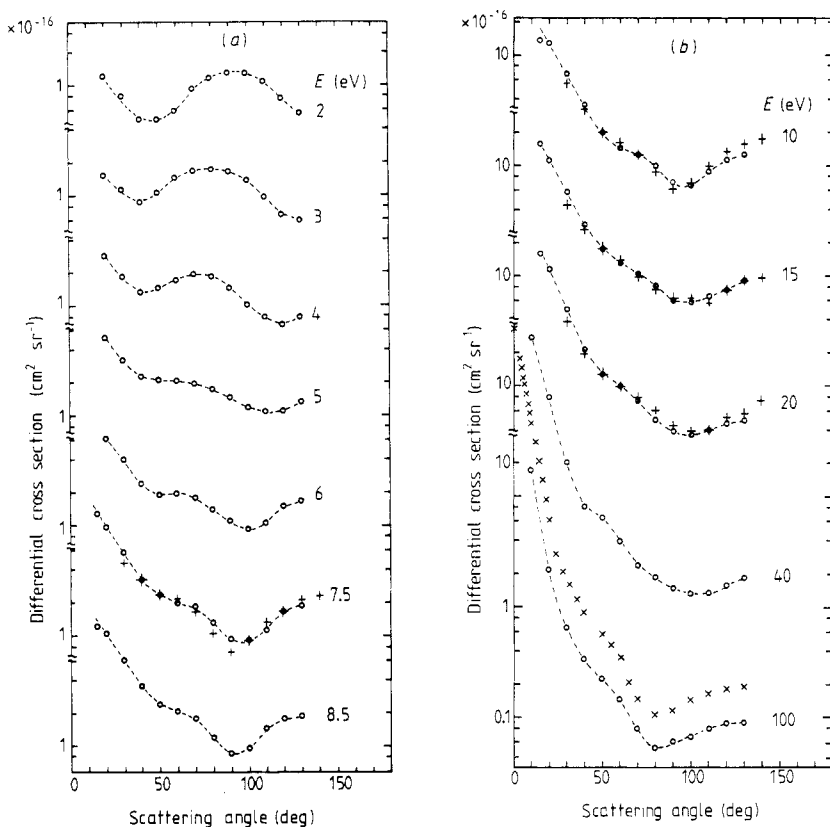
Following the above procedures very carefully, we measured the DCS at 2, 3, 4, 6, 7.5, 8.5, 10, 15, 20, 40 and 100 eV for scattering angles of  $10/15^\circ$ , and from  $20^\circ$  to  $130^\circ$  in steps of  $10^\circ$ . The energy resolution in these measurements (reduced to 40–50 meV to obtain stronger electron beams) was not high enough to resolve the vibrational excitation in the  $\nu_4$  mode and the pure rotational excitation. The intensity  $I$  of the full elastic peak was obtained by a numerical integration over all channels extending to  $\pm 0.1$  eV on both sides of the peak. The He standard was derived from the data of Andrick and Bitsch (1975) except for impact energies of 20, 40 and 100 eV where the fitted values of Register *et al* (1985) were used. Values at 7.5 and 8.5 eV are linear interpolations. The resulting normalised cross sections of  $C_2H_6$  are given in table 1. Error estimates are as follows: drifts in the incident electron beam as observed by a Faraday cup before and after the measurements were less than 5%, errors of pressure and Poisson errors are about 5%. Contributions from the background pressure are negligible (measured), and contributions from the vibrational excitation  $\nu_4$  are at most 1%. Finally, errors due to an asymmetric definition of the angular 'zero' are estimated to be less than 5%. Combination of these instrumental errors with the uncertainty of the reference He cross sections (5–20%) leads to a total error of the order of 15–22%.

Figure 1 shows the DCS as a function of scattering angles and incident energies. Previous experimental data of Curry *et al* (1985) and Fink *et al* (1975) are included. Curry's relative angular distributions were normalised to the present DCS at  $\theta = 50^\circ$ . In general, the agreement is excellent. However, at 100 eV, our values are lower by a factor of two and the shape differs from that of Fink.

Fully aware of the theoretical insufficiencies, we have parametrised the experimental angular distributions with a modified phaseshift fit (cf Tanaka *et al* 1982). This includes polarisation correction and Thompson–Born estimates of the higher partial waves. If a reasonable fit is obtained it can serve as a first approximate extrapolation to  $0^\circ$  and  $180^\circ$ . Four phases plus a size factor were sufficient in the lower energy ranges, but beyond 20 eV six phases are required. At 40 eV, a fictitious 'point' was added to the

Table 1. Differential and integral cross sections in units of 10<sup>-16</sup> cm<sup>2</sup> sr<sup>-1</sup>.

eV θ (deg)		2	3	4	5	6	7.5	8.5	10	15	20	40	100
10	—	—	—	—	—	—	—	—	—	—	—	25.12	17.87
15	—	—	—	—	—	—	12.90	12.02	13.36	15.46	15.90	—	—
20	1.235	1.543	2.809	5.217	6.223	6.223	9.555	10.49	12.77	11.02	11.35	7.910	2.158
30	0.795	1.166	1.878	3.249	4.048	4.048	5.732	6.163	6.686	5.668	4.936	2.001	0.652
40	0.487	0.871	1.335	2.270	2.406	2.406	3.260	3.507	3.575	2.898	2.108	0.806	0.337
50	0.493	1.060	1.485	2.129	1.921	1.921	2.359	2.361	1.964	1.730	1.259	0.638	0.220
60	0.678	1.450	1.734	2.083	1.950	1.950	2.011	2.103	1.416	1.291	0.995	0.370	0.144
70	0.929	1.696	1.956	1.950	1.792	1.792	1.831	1.787	1.252	1.026	0.731	0.236	0.079
80	1.173	1.728	1.828	1.738	1.417	1.417	1.321	1.212	0.963	0.801	0.482	0.199	0.051
90	1.242	1.652	1.422	1.453	1.113	1.113	0.924	0.834	0.699	0.591	0.380	0.169	0.061
100	1.240	1.340	1.015	1.181	0.924	0.924	0.893	0.941	0.645	0.577	0.358	0.147	0.067
110	1.048	0.947	0.794	1.063	1.055	1.055	1.132	1.452	0.871	0.650	0.404	0.142	0.079
120	0.754	0.666	0.672	1.087	1.488	1.488	1.660	1.726	1.119	0.740	0.448	0.172	0.088
130	0.655	0.585	0.788	1.309	1.636	1.636	1.852	1.835	1.240	0.909	0.480	0.193	0.090
σ <sub>i</sub>	10.82	14.71	19.13	24.34	26.76	26.76	31.68	30.11	28.75	25.26	21.82	14.10	6.600
σ <sub>M</sub>	9.74	12.10	15.78	19.82	22.20	22.20	23.48	20.10	16.25	10.88	6.99	3.76?	1.41?



**Figure 1.** Differential cross sections for elastic scattering of electrons by  $\text{C}_2\text{H}_6$ . The data (○) are connected by hand-drawn broken curves to help in the visualisation. Also shown are the measurements of Curry *et al* (1985) (+) and Fink *et al* (1975) (x).

data set at  $180^\circ$  in order to constrain the fit at large angles. Obviously the fits miss some of the finer details in the data, but represent the general shape rather well. The product of phase  $\delta_0$  and size factor behaves similarly to the total cross section, see below, while the other phases are small and nearly constant for 2–4 eV, then increase between 5–10 eV and become rather flat again beyond 10 eV with small increases in  $\delta_3$  and  $\delta_4$  with energy. The phases at 100 eV belong to a different pattern. The trends in the phase pattern agree with a visual inspection of the angular distributions. At low energies (2–4 eV) the pattern is typical for a strong d wave and the fits are excellent. From about 6–7.5 eV on, a well distinguishable f-wave pattern sets in and remains visible until 20 eV, and interestingly, can also be observed in the 100 eV data (see also Fink *et al* (1975) and/or the theoretical data of the independent-atom model). Around 40 eV the pattern is more obscure, though. The characteristic behaviour in the region from 6–8 eV was also observed by Matsunaga *et al* (1981) and Curry *et al* (1985).

Integral and momentum transfer cross sections were obtained from the parametrised fits and show a very consistent behaviour, cf figure 2.  $\sigma_1$  is practically independent of the number of parameters. The integrals are included at the bottom of table 1 and are compared with other measurements in figure 2. On a logarithmic scale, the slow drop in  $\sigma_1$  after the peak at 7.5 eV becomes almost linear up to 100 eV. Most remarkable is the excellent agreement with the old total cross section measurements of Brüche

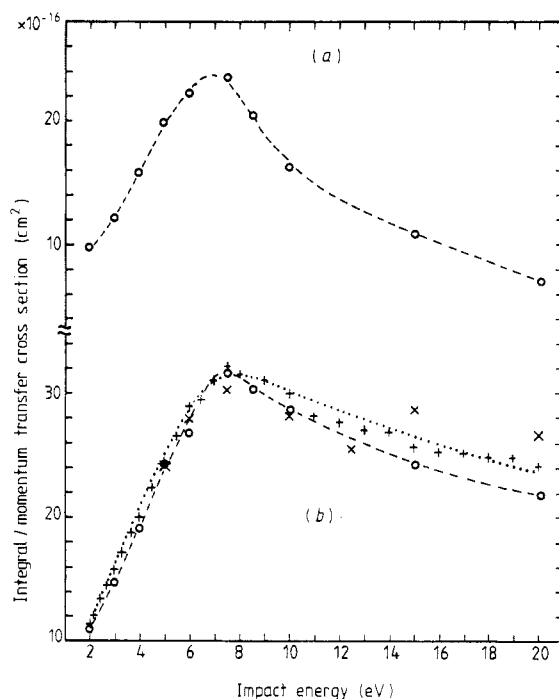


**Figure 2.** Integral (b) and momentum transfer (a) cross sections of figure 1 calculated from the phaseshift fits (broken curves). Included are the data of Brüche (1930) ( $\cdots$ ), Floeder *et al* (1985) ( $\times$ ), and Sueoka and Mori (1986) (+).

(1930) and the more recent data of Floeder *et al* (1985) and Sueoka and Mori (1986).  $\sigma_M$  depends more strongly on the number of parameters ( $\pm 15\%$ ?) due to the different shape of the fits beyond  $130^\circ$ . An estimate of  $\sigma_M$  near 2 eV obtained from electron swarm transport parameters (Duncan and Walker 1974) is about twice as large as our value.

Ethane belongs to the  $D_{3d}$  point group. Its ground-state electron configuration is  $(C_{\text{core}})^4 - 2a_{1g}^2 2a_{2u}^2 1e_u^4 3a_{1g}^2 1e_g^4$  yielding the  $\tilde{X}^1A_{1g}$  ground-state symmetry. The lowest unoccupied orbitals are  $a_{1g}$ ,  $e_g$ ,  $a_{2u}$  and  $e_u$  (cf Caldwell and Gordon 1978), the two lowest allowed states are  $1^1A_{2u}$  and  $1^1E_u$  whose excitation energies correspond to the experimentally observed transition of 9.4 eV (Lasette *et al* 1969, Johnson *et al* 1979). The two optically forbidden levels ( $1^3E_g$  and  $1^3A_{1g}$ ) have small cross sections—and so far, have not been clearly observed (however see Wang 1982). According to the angular correlation theory (Read 1968, Andrick and Read 1971) the symmetry of these levels allows only the angular moments of  $l=0$ ,  $l=2$  for  $A_{1g}$ , and  $l=2$ ,  $l=4$  for  $E_g$ , while the two next states, i.e.  $A_{2u}$  and  $E_u$  both have quantum numbers  $l=1$  and  $l=3$ . Thus, if the broad peak seen in the total cross sections  $\sigma_I$  and  $\sigma_M$  near 7.5 eV is a short-lived shape resonance and, given the observed f-wave behaviour, we have to assume that the dominant shape resonance most probably is a  $^2A_{2u}/^2E_u$  state with incident electrons trapped in the  $a_{2u}$  or  $e_u$  orbitals (the two levels are only 0.05 eV apart). This is confirmed from the analogy with similar results for CH<sub>4</sub> (Tanaka *et al* 1982) and from the observation of only a single broad peak in our preliminary measurements of the vibrational excitation. The dominant partial waves of this resonance are then f and p with the former characterising the angular distribution.

With decreasing incident energies the local 'maximum' at 50–60° in the 7.5 eV distribution becomes more prominent and shifts towards higher angles until at 2 eV clear minima at 50° and 130° appear which are arranged symmetrically around 90°, i.e. a strong  $l=2$  behaviour. However, the total cross sections show no structure until the onset of the Ramsauer–Townsend minimum. This suggests that the contribution of non-resonant direct scattering arising from the  $^1A_{1g}$  state contains mainly  $l=0$  and  $l=2$ , wave scattering determining the DCS. As to be expected, at energies above 10 eV the spectral variation becomes more gradual and the angular distribution increases progressively in the forward direction since the electron transfers less and less momentum to the target.

#### 4. Conclusion

The present work provides a self-consistent set of quantitative differential cross sections for e-C<sub>2</sub>H<sub>6</sub> vibrationally elastic scattering together with the corresponding integral and momentum transfer cross sections. Although there remain errors of the order of 15–22%, we are confident that we have obtained more accurate results than our previous data. We are presently investigating the corresponding vibrationally inelastic scattering cross sections and will report them separately.

#### References

- Abusalbi N, Eades R A, Nam T, Thirumalai D, Dixon D and Truhlar D G 1983 *J. Chem. Phys.* **78** 1213  
Andrick D and Bitsch H 1975 *J. Phys. B: At. Mol. Phys.* **8** 393  
Andrick D and Read F H 1971 *J. Phys. B: At. Mol. Phys.* **4** 389  
Boesten L 1988 *Rev. Sci. Instrum.* in press  
Brinkmann R T and Trajmar S 1981 *J. Phys. E: Sci. Instrum.* **14** 245  
Brüche R B 1930 *Ann. Phys., Lpz* **4** 387  
Caldwell J W and Gordon M S 1978 *Chem. Phys. Lett.* **59** 403  
Chutjian A 1979 *Rev. Sci. Instrum.* **50** 347  
Curry P J, Newell W R and Smith A C H 1985 *J. Phys. B: At. Mol. Phys.* **18** 2303  
DiChio D and Natali S V 1974 *Rev. Sci. Instrum.* **45** 559, 566  
Duncan C W and Walker I C 1974 *J. Chem. Soc. Faraday Trans. II* **70** 577  
Fink M, Jost K and Herrmann D 1975 *J. Chem. Phys.* **63** 1985  
Floeder K, Fromme D, Raith W, Schwab A and Sinapio G 1985 *J. Phys. B: At. Mol. Phys.* **18** 3347  
Gianturco F A and Thompson D G 1976 *J. Phys. B: At. Mol. Phys.* **9** L383  
— 1980 *J. Phys. B: At. Mol. Phys.* **13** 613  
Johnson K E, Kim K, Johnston D B and Lipsky S 1979 *J. Chem. Phys.* **70** 2189  
Kimura M, Sato H and Fujima K 1987 private communication  
Kisker E 1983 *Rev. Sci. Instrum.* **54** 1113  
Kisker E, Clauberg R and Gudat W 1982 *Rev. Sci. Instrum.* **53** 1137  
Lasette E N, Skerbele A and Dillon M A 1969 *J. Chem. Phys.* **49** 2382  
Matsunaga D, Kubo M and Tanaka H 1981 *Proc. 12th Int. Conf. on the Physics of Electronic and Atomic Collisions (Gatlinburg)* ed S Datz (Amsterdam: North-Holland) abstracts p 358  
Olander D R and Kruger V 1970 *J. Appl. Phys.* **41** 2769  
Read F H 1968 *J. Phys. B: At. Mol. Phys.* **1** 893  
Register D F, Trajmar S and Srivastava S K 1985 *Phys. Rev. A* **21** 1134  
Rohr K 1980 *J. Phys. B: At. Mol. Phys.* **18** 4897  
Srivastava S K, Chutjian A and Trajmar S 1975 *J. Chem. Phys.* **63** 2659  
Sueoka O and Mori S 1986 *J. Phys. B: At. Mol. Phys.* **19** 4035  
Tanaka H and Boesten L 1988 to be published



- Tanaka H, Kubo M, Onodera N and Suzuki A 1983 *J. Phys. B: At. Mol. Phys.* **16** 2861
- Tanaka H, Okada T, Boesten L, Suzuki T, Yamamoto T and Kubo M 1982 *J. Phys. B: At. Mol. Phys.* **15** 3305
- Trajmar S and Register D F 1985 *Electron-Molecule Collisions* ed I Shimamura and K Takayanagi (New York: Plenum) p 427
- Wang R G, Dillon M A, Spence D and Wang Z W 1982 *Argonne National Laboratory, Radiological and Environmental Research Division, Annual Report ANL-82-65* Part I, Oct. 1981-Dec. 1982, p 45